ANL-06/55

Argonne NATIONAL LABORATORY

Beam Intensity Expectations for a 200 MeV/u 400 kW Radioactive Beam Driver Accelerator

Physics Division

About Argonne National Laboratory

Argonne is a U.S. Department of Energy laboratory managed by UChicago Argonne, LLC under contract DE-AC02-06CH11357. The Laboratory's main facility is outside Chicago, at 9700 South Cass Avenue, Argonne, Illinois 60439. For information about Argonne, see www.anl.gov.

Availability of This Report

This report is available, at no cost, at http://www.osti.gov/bridge. It is also available on paper to the U.S. Department of Energy and its contractors, for a processing fee, from:

U.S. Department of Energy
Office of Scientific and Technical Information
P.O. Box 62
Oak Ridge, TN 37831-0062
phone (865) 576-8401
fax (865) 576-5728
reports@adonis.osti.gov

ANL-06/55

Beam Intensity Expectations for a 200 MeV/u 400 kW Radioactive Beam Driver Accelerator

by
B.B. Back and C.L. Jiang
Physics Division, Argonne National Laboratory

November 14, 2006

A U.S. Department of Energy laboratory managed by UChicago Argonne, LLC

Beam intensity expectations for a 200 MeV/u 400 kW radioactive beam driver accelerator

B. B. Back and C. L. Jiang

Argonne National Laboratory

Argonne, Illinois 60439, USA

(Dated: November 14, 2006)

Abstract

The expected radioactive ion production rate for a 200 MeV/u 400 kW driver linac usingfour different production methods is discussed. For each isotope the optimum method is identified and the rate is calculated based on different model assumptions, empirical observation and extrapolations. The results are compared to the rates expected for a 550 MeV proton driver machine with a beam power of 50 kW, as well as the full RIA facility with a 400 MeV/u 400 kW production linac.

PACS numbers: 29.17.+w, 29.25.Rm

I. INTRODUCTION

The full Rare Ion Accelerator (RIA) project is based on a superconducting linac which is capable of providing production beams ranging from about 1 GeV protons to 400 MeV/u U beams with a total power of 400 kW. The scientific merit of this facility is presently under review by the Rare Ion Science Advisory Committee (RISAC) [1] of the National Academy of Sciences. The present work represents an evaluation of the ion production capabilities of a facility based on a scaled down production accelerator with roughly half the beam energy but increased beam intensity, such that the full 400 kW beam power will still be available for isotope production. The production mechanism considered include only those needed for generating ions for re-acceleration, thus excluding the in-flight beam capability of the full RIA project. In order to evaluate the competitiveness of such a facility against other international re-accelerated beam facilities, a direct comparison of beam intensities relative to those expected for a 50 kW 550 MeV proton driver beam has been carried out. These parameters roughly correspond to those of the planned ISAC-II facility at the Tri-University Meson Facility (TRIUMF) in Vancouver, Canada, which is expected to be the closest competitor in this area.

II. MACHINE CONFIGURATION

The machine configuration represent a shortened version of the Argonne version of the RIA driver linac. Instead of using 302 superconducting resonators in RIA, only 221 resonators comprise the driver linac in the scaled-down facility, here denoted AEBL for Advanced Exotic Beam Laboratory. Recent developments in heavy-ion ECR source technology [2] allows for a design with a factor two higher beam currents such that the total beam power is unchanged from the RIA design. The radioactive ion production rates discussed in the following are thus based on a driver linac capable

of providing the primary beams listed in Table. I [3]. The ion yields are all estimated under the assumption that the appropriate target technology capable of withstanding this beam power is available or can be developed.

TABLE I: Representative beams from a 200 MeV 400kW superconducting driver linac [3]

Beam	Energy (MeV/u)	Power (kW)
proton	550	400
^{3}He	385	400
deuteron	319	400
^{18}O	280	400
^{40}Ar	275	400
^{86}Kr	250	400
^{136}Xe	230	400
^{238}U	200	400

III. PRODUCTION METHODS

The production methods fall into two categories, namely those based on thick targets from which the ions are subsequently extracted by diffusion/effusion and ionized in an ion source, Fig. 1b, and those in which reaction products are brought to rest in a gas cell and extracted for further manipulation, Fig. 1a. The following four subsections discusses each production method separately and lists the relevant model assumptions and empirical information on which the rate estimates are based.

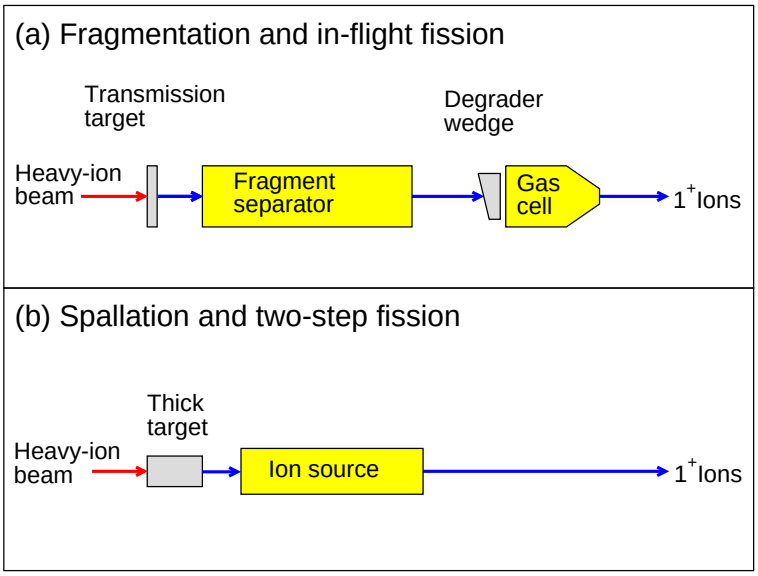

FIG. 1: Concepts for production of radioactive 1^+-ions using in-flight methods (fragmentation and in-flight fission) and diffusion/effusion from thick targets (spallation and two-step fission).

A. Proton and ^{3}He induced spallation

Much experience has been gained using this production method at the Isotope Separator On-Line (ISOLDE) at CERN over the last several decades. An extensive set of data [4] on the extracted beam intensities is available for a very wide range of beams produced at this facility. This method is most productive for elements that diffuse rapidly out of the production target. For isotopes listed in the ISOLDE-SC database, we have thus used the observed production rates scaled appropriately with the available beam intensity to estimate the rates for the driver accelerator under consideration. Simple exponential extrapolations were done for elements for which a sufficient range of isotopic yields are listed in the ISOLDE-SC database. Corrections for decays occuring during the efusion/diffusion from the target, especially important for short-lived isotopes, were applied using extraction times measured for neutron

induced fission of ^{235}U [9]. This method of extrapolation was used for the following elements: F, Ne, Na, K, Ni, Cu, Zn, As, Br, Kr, Rb, Sr, Cd, In, Sb, I, Xe, Cs, Ba, Sm, Eu, Gd, Tb, Dy, Ho, Er, Tm, Yb, Lu, Hg, Tl, Rn. For elements not measured by Rudstam *et al.* we used extraction time parameters for another element in the same group in the periodic table. Tha same exttrapolation method was used in Ref. [14].

For the remaining elements, extrapolations to very neutron-rich and neutron-poor isotopes were based on the isotopic distribution of production rates suggested by Lukic *et al.* [5]. This work lists the Gaussian width and centroid of isotopic distributions ions produced at CERN ISOLDE with the 600 MeV proton beam and provides an analysis of the effects of the ion-source release time in relation to the half-life of short lived species. Based on this information we have extrapolated the expected yield for exotic isotopes of C,N, O, Mg, Al, Cl, Ar, Ca, Sc, Mn, Ga, Ge, Se, Y, Pd, Ag, Sn, Te, La, Ce, Pr, Nd, Pm, Hf, Pb, Bi, Po, At, Fr, and Ra. For elements, for which more abundant isotopes have been observed at CERN, but the release-time is not listed in Ref. [5], we assume a release time of 400 s. The data shown in Figs. 2-4 therefore include effects of decays that occur before the 1^+ ions reach the ion source for this production mechanism. Note that this extrapolation method differs from that used in Ref. [14]

B. Two-step fission

The two-step fission method separates the beam-stopping Ta target from the UCx target, in which the radioactive ions are produced by neutron-induced fission via neutrons from deuteron bombardment of the central Ta target [6]. Since no direct experimental data are available on the production rate using this method, we rely exclusively on model calculations using the LAHET/MCNPX codes [7, 8]. The results have been corrected for decay during the release from the production target using the method and parameters of Rudstam *et al.* [9]. Where no life-time data are available

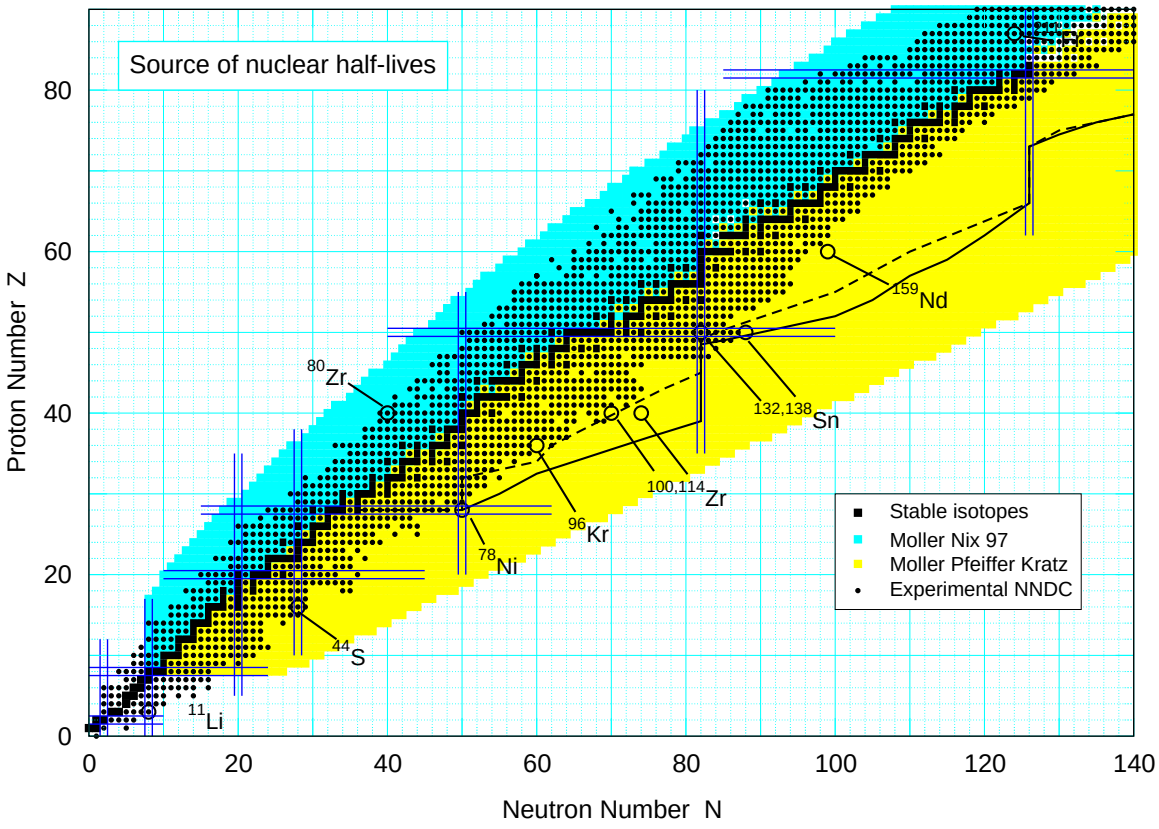

FIG. 2: Source of halflife sources used for corrections.

we use predictions from Ref. [10]. The estimate of the two-step fission production rates thus mirror those described in Ref. [14].

C. Projectile fragmentation

A substantial amount of experiential data on this production mechanism have been accumulated at modern beam fragmentation facilities at GSI, Ganil and NSCL as summarized in the phenomenological EPAX model [11, 12]. We have used this model to estimate the production rate in projectile fragmentation except for the fragmentation of Th and U projectiles. In these cases some parameters in the model were adjusted to better reproduce observed production yields [13]. Since the model

predicts only the production rate of isotopes flying out of the target, it is necessary to apply several efficiency factors in order to estimate the rate of 1^+ ions available for re-acceleration. The 1+ rate is therefore given as

$$R_{1+} = R_{tgt} \times P_q \times t_{FS} \times t_W \times t_{GC} \times S_{GC}, \quad (1)$$

where rate out of the target R_{tgt} is reduced by the following factors: P_q, the population of charge state q, t_{FS}, the transmission through the fragment separator assumed to have a solid angle of $\Delta\Omega$= 10 msr and a momentum acceptance of $|\Delta p/p| \leq 9\%$, t_W, the transmission through an degrader wedge (assumed to be 100%), t_{GC}, the transmission through the gas cell (assumed to be 20%), and $S_{GC} = \exp(-T_{GC}/T_{1/2})$, which takes into account the decay losses during the assumed T_{GC}=20 ms residence time in the gas cell. In addition, the ion transmission rate through the gas cell is limited to 10^9 ions/sec. Although this upper limit is not known experimentally at this time, it is expected that the ionization density of the He gas will result in a screening of the longitudinal electric field that forces the ions toward the exit leading to a reduction of the transmission. The same limit was imposed on calculations presented in Ref. [14]. Note, however, that the correction for decay losses in the gas cell, S_{GC}, was not included in Ref. [14].

D. In-flight fission

This production mechanism is based on the fission decay of ^{238}U nuclei as they interact with a thin target e.g. a flowing thin sheet of liquid ^{7}Li. Estimates of the production rates were based on experimental data from GSI [15] and calculations using the PROFI model [16] were also used. As for the fragmentation method, the rates were corrected for the charge state population, mass separator, wedge, and gas cell transmission as well as the decays occuring during the gas cell residence time. The lower ^{238}U beam energy as compared to the RIA facility especially affect the

mass separator transmission because of the kinematics of the fission process. Note, that the present estimates differ from those of Ref. [14] by including the correction for decay losses in the gas cell, S_{GC}.

IV. RESULTS

The yields of 1^+ ions available for charge state breeding and acceleration are shown in Fig. 3 as a color map as a function of neutron number, N and atomic number Z. Detailed plots for the production of individual elements are given in the Appendix. The location of single-particle shell closures at N, Z=2,8,20,29,50, and 82 are indicated by solid blue lines and the location of some specific isotopes are indicated for orientation. The solid and dashed black lines represent two different estimates of the location of the main r-process path.

V. BEST REACTION MECHANISM

Figure 4 gives a color map representation of the optimum reaction for producing specific isotopes. We observe that a very wide range of isotopes can be produced by the projectile fragmentation process (yellow), but that more specialized reactions, such as the proton/^{3}He spallation process (orange), the in-flight fission (red), and the two-step fission (brown) methods are more efficient in certain limited regions of the $N-Z$ chart. Only species with a predicted production rate exceeding 10^{-4} part/sec are included in this comparison.

VI. COMPARISON TO 50 KW ISOL FACILITY

Figure 5 represents a comparison of the predicted production rate for the 200 MeV/u 400 kW driver accelerator considered here to a 550 MeV proton driver with 50

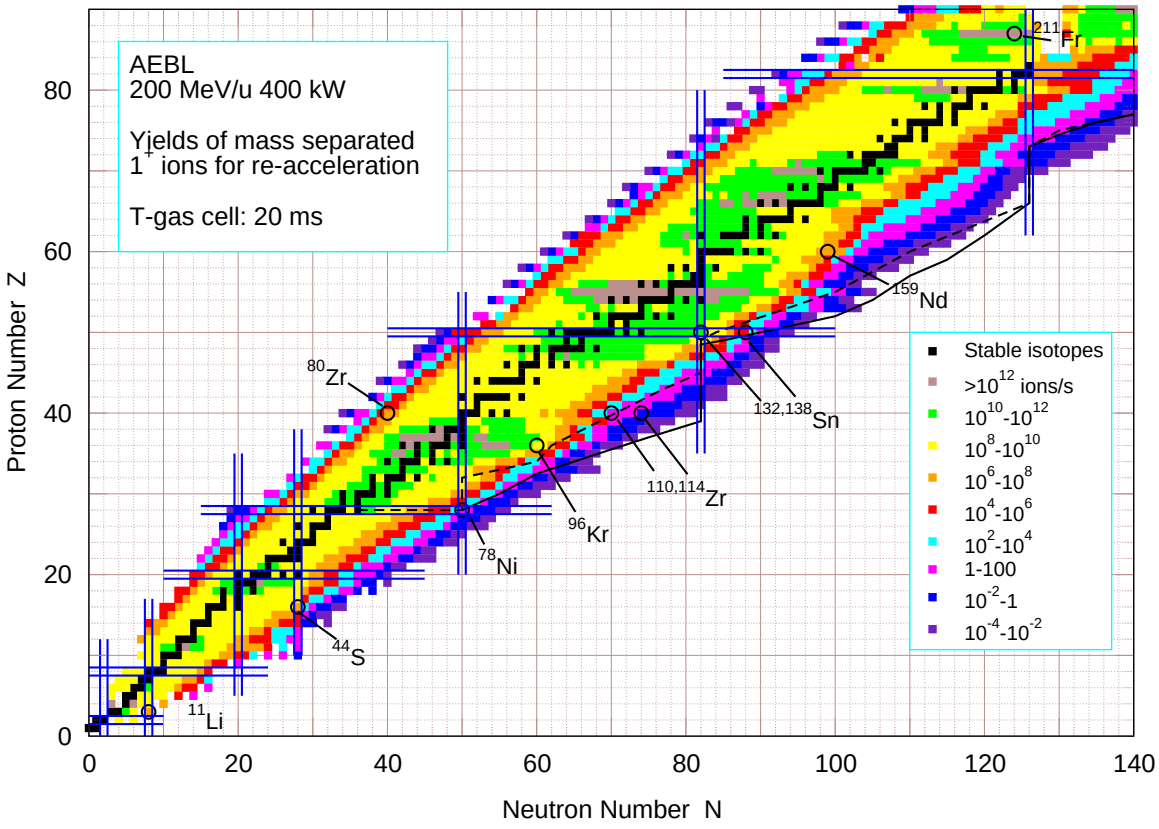

FIG. 3: Yields for production of radioactive 1^+-ions in a 200 MeV/u 400 kW machine.

kW beam power using only the spallation reaction in the thick target using the same calculations. Such a facility corresponds roughly to the planned ISAC-II upgrada at TRIUMF. Isotopes indicated by a blue square with a central white dot are those for which the optimum reaction mechanism is proton spallation. The expected production ratio of eight therefore only reflect the increase in beam power from 50 kW to 400 kW. Isotopes, for which the production in the present machine exceed that of the 50 kW spallation driver by a factor between 10 to 1000 are indicated by a cyan color, whereas the yellow areas are isotopes produced at a rate more than 1000 times that of the spallation machine. From this comparison it is clear that there is a very large range of isotopes for which the present machine provides a very substantial advantage

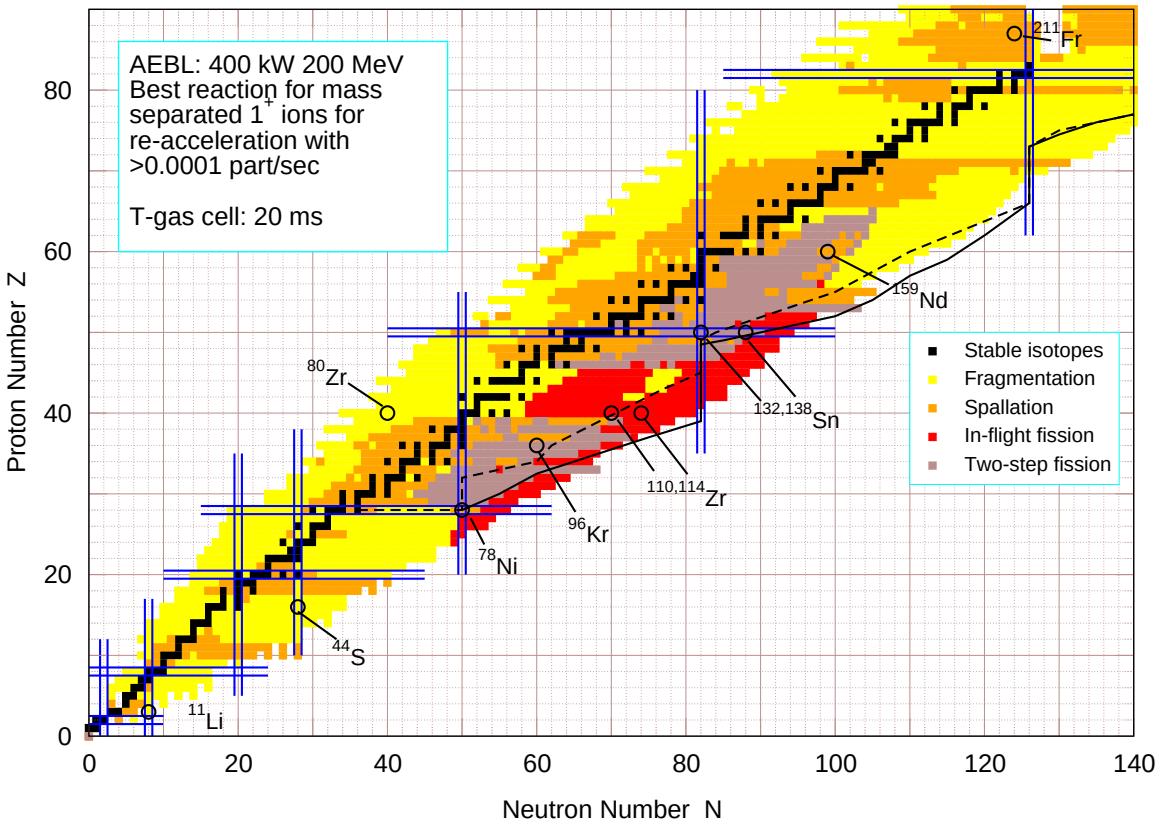

FIG. 4: Map of the optimum reaction mechanism for production of radioactive 1^+-ions in a 200 MeV/u 400 kW machine.

over competing technologies.

VII. COMPARISON TO THE FULL RIA FACILITY

It is of interest to compare the present calculations for a 200 MeV/u 400 kW production linac to those considered earlier for a 400 MeV/u facility with the same beam power. It is evident that for the majority of beam specied the production yield for the 20 MeV/u maching matches that of the 400 MeV/u facility because the beam power is the overriding factor, see Fig. 6. As expected, the 200 MeV machine loses

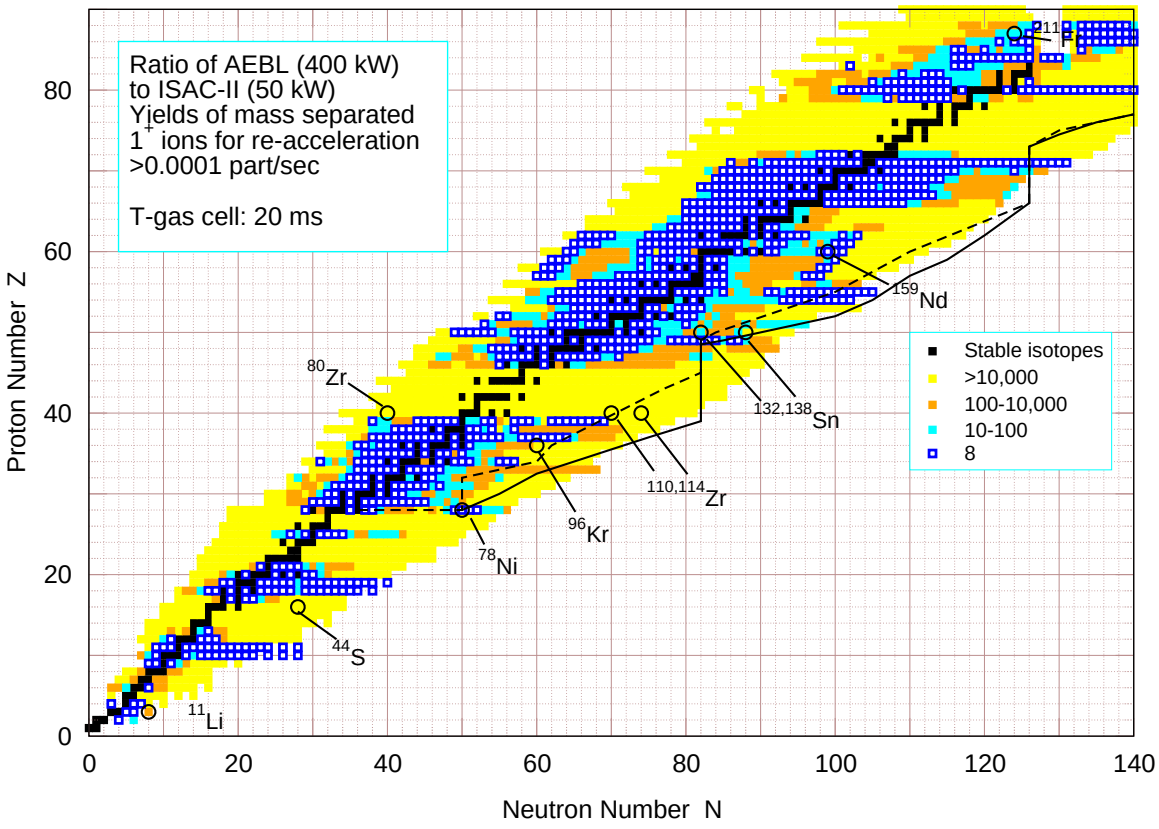

FIG. 5: Comparison of production rates of radioactive 1^+-ions in a 200 MeV/u 400 kW machine to that expected for ISAC.

some intensity for the most unstable beams as indicated by the yellow areas. There is, however, a significant range of beams, namely those that are optimally produced by in-flight fission [14], for which the yield drops off by more than an order of magnitude. This effect is caused by the fact that the opening angle of in-flight fission fragments increases significantly as a consequence of the lower velocity of the fissioning ^{238}U beam to the extend that it exceeds the angular acceptance of the fragment mass analyzer.

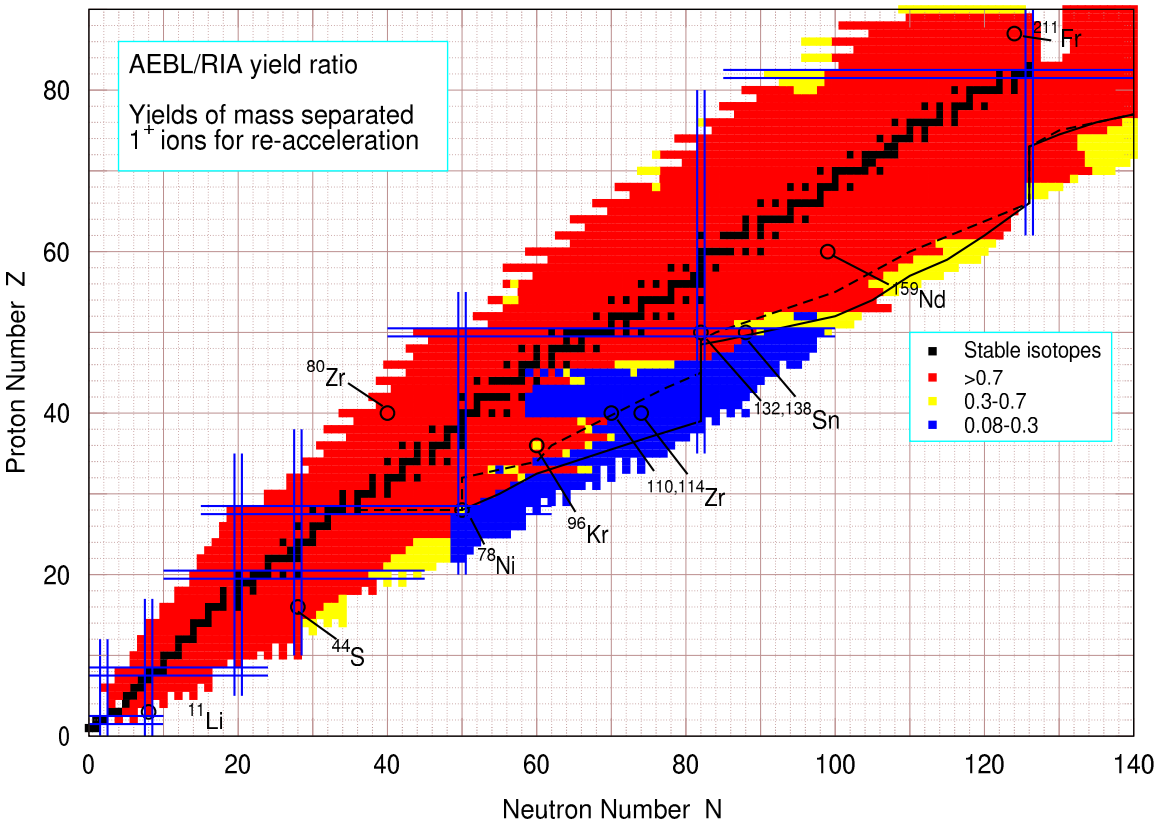

FIG. 6: Comparison of production rates of radioactive 1^+-ions in a 200 MeV/u 400 kW machine to that expected for the full RIA facility with 400 MeV/u 400 kW driver beams.

VIII. SUMMARY

The production capability of 1^+ ions for re-acceleration of a nominal 200 MeV/u superconducting driver linac capable of accelerating 550 MeV protons and 200 MeV/u ^{238}U nuclei with a total beam power of 400 kW has been evaluated. These results are compared with those expected for a 50 kW spallation facility using only proton beams of 550 MeV. A direct comparison of these two facilities reveal a substantial superiority of the former facility which produces beams for a very wide range of the most interesting nuclei that exceed those of the latter by more than three orders of

magnitude. No other planned facility will provide these intense re-accelerated beams obtained from stopping of fast fragments. A comparison with the full RIA facility, with a 400 MeV/u 400 kW production linac, shows that only beams produced by the in-flight fission method suffer noticable yield reductions, an effect caused by the increase in opening angle of the fission fragment emission resulting from the lower beam velocity.

Acknowledgment

This work was supported by the U.S. Department of Energy, Office of Nuclear Physics, under Contract No. DE-AC02-06CH11357.

---

[1] Rare Ion Sciences Advisory Committee:http://www7.nationalacademies.org/bpa/RISAC.html

[2] D. Leitner and C.M. Lyneis, in proceedings of the Knoxville 2005, Particle Accelerator Conference, Knoxville, Tennessee, Knoxville, Tennessee, 16-20 May 2005. p. 179.

[3] P. Ostroumov, private communication

[4] SC Isolde Production Yields, http://www94.web.cern.ch/ISOLDE/

[5] S.Lukic *et al.*, nucl-ex/0601031

[6] J.Nolen *in proceedings of* Third International Conference on Radioactive Nuclear Beams, East Lansing, MI, May 24-27, 1993, p.111.

[7] R.G.Alsmiller *et al.*, Nucl. Instr. Meth. **A 278**, 713 (1989)

[8] MCNPX 2.1.5 User's Manual in: L.Waters (Ed.), Report LA-UR 99-6058, Los Alamos National Laboratory, Nov 1999.

[9] G. Rudstam *et al.*, Radio Chim. Acta **49**, 155 (1990).

[10] P. Möller *et al.*, At. Data Nucl. Data Tables **66**, 131 (1997).

[11] K. Sümmerer, W. Brüchle, D.J. Morrissey, M. Schädel, B.Szweryn, and Y. Weifan, Phys. Rev. **C42** (1990) 2545.

[12] K. Sümmerer and B. Blank, Phys. Rev. **C61**(2000) 034607.

[13] M. Pfützner, Phys. Lett. **B444** (1998) 32; A.R. Junghans, DISS. **98-07**, March 1998, GSI; A.R. Junghans et al., Nucl. Phys. **A629** (1998) 635.

[14] C.L.Jiang *et al.*, Nucl. Instr. Meth. **A492**, 57 (2002)

[15] C.O. Engelmann, Diss. **98-015**, 1998, Gesellschaft für Schwerionenforsching, Darmstadt, Germany.

[16] J. Benlliure *et al.*, Nucl. Phys. **A628** (1998) 458

IX. APPENDIX

This appendix presents the expected yields for 1^+ ions for the 200 MeV/u 400kW machine shown for all elements from Hydrogen to Thorium organized with six elements per figure.

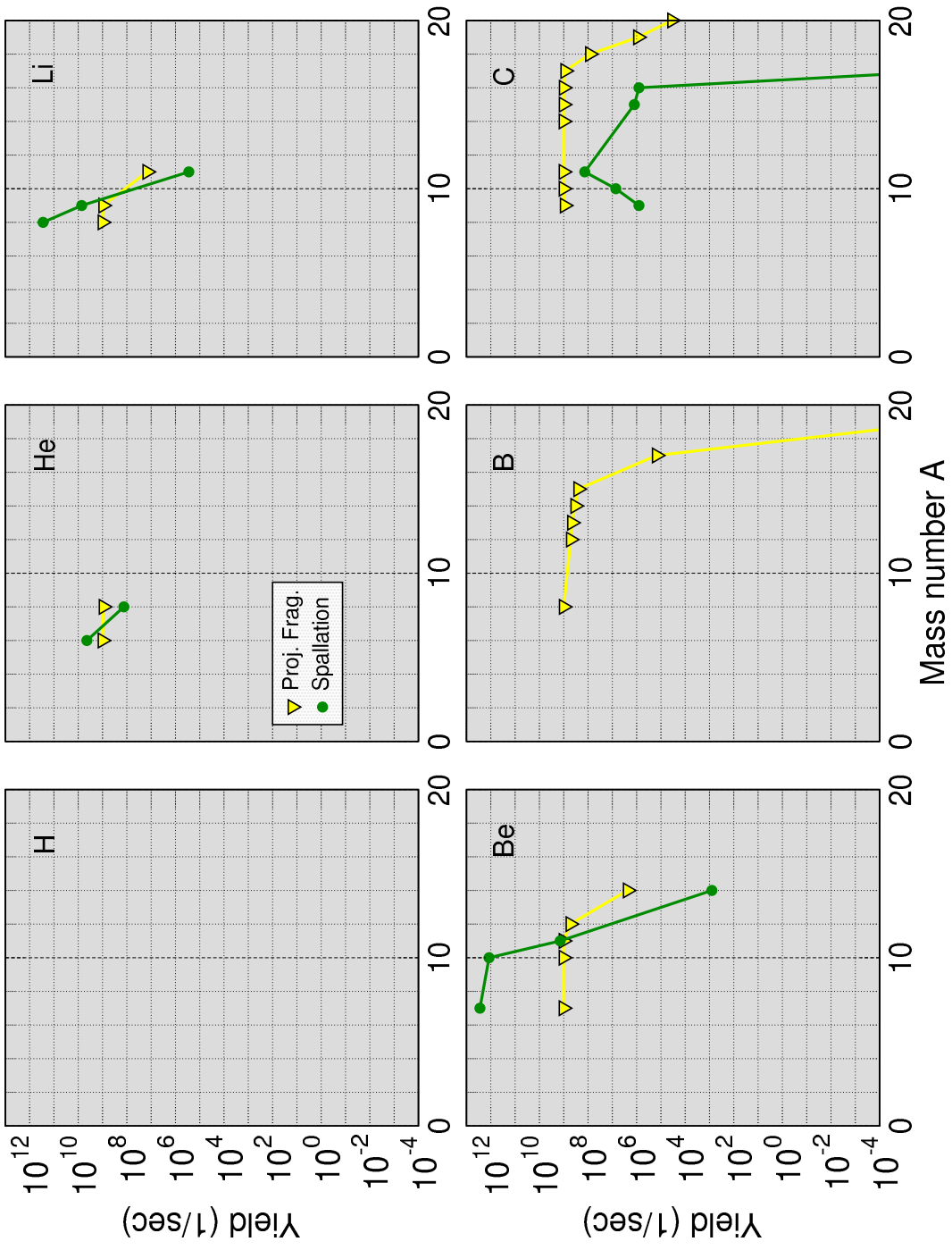

FIG. 7: Production rates of H, He, Li, Be, B, C 1^+-ions in a 200 MeV/u 400 kW machine.

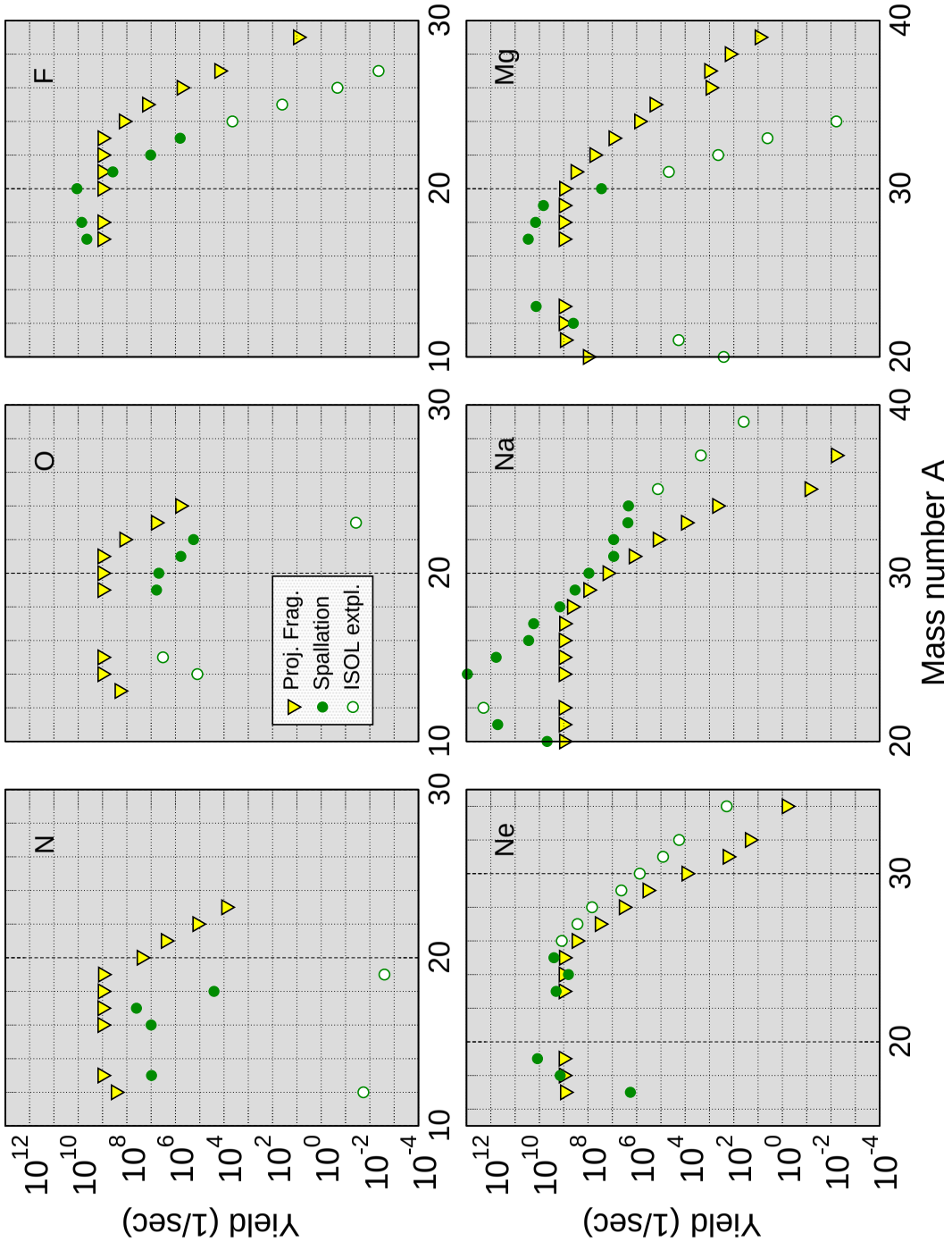

FIG. 8: Production rates of N, O, F, Ne, Na, Mg 1^+-ions in a 200 MeV/u 400 kW machine.

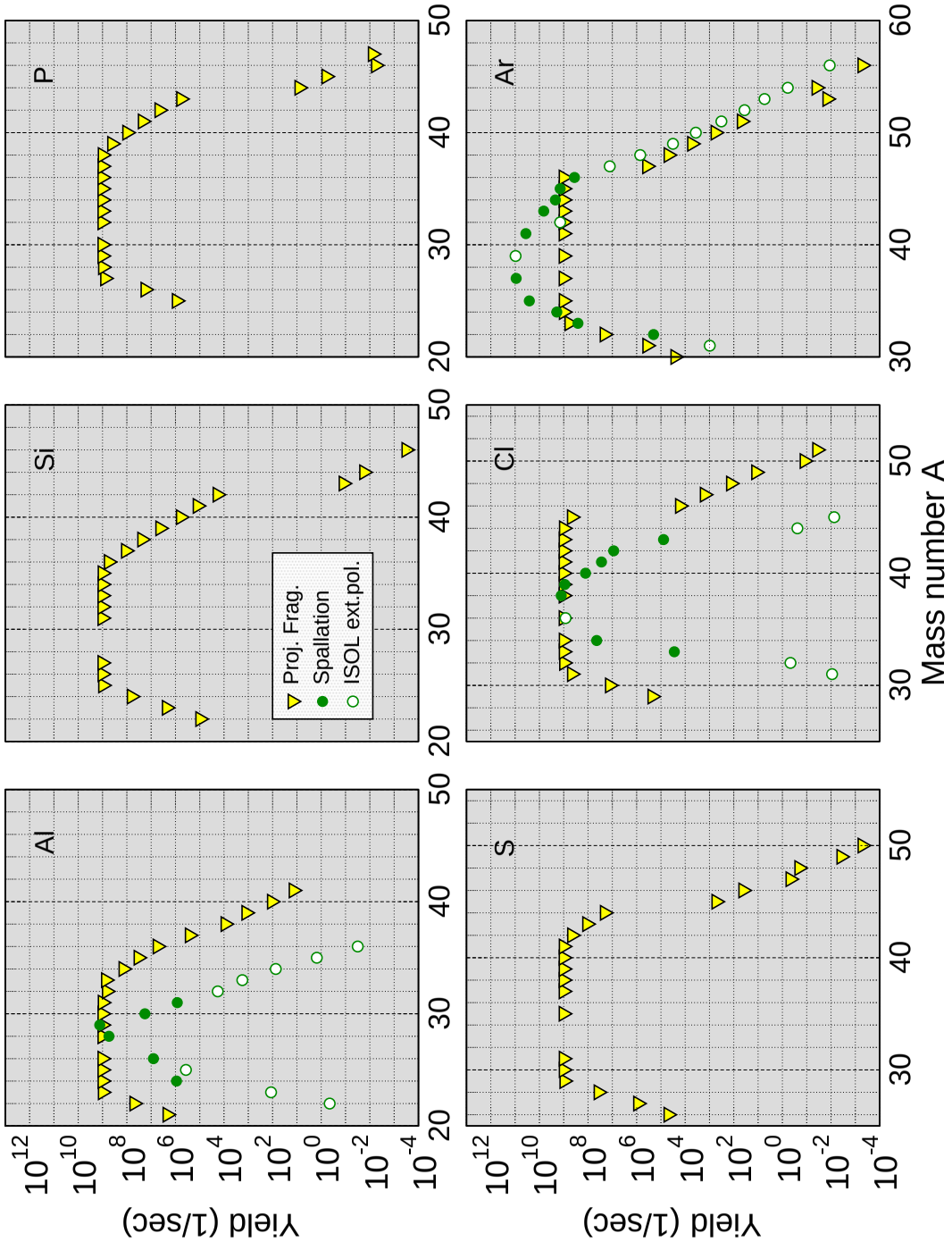

FIG. 9: Production rates of Al, Si, P, S, Cl, Ar 1^+-ions in a 200 MeV/u 400 kW machine.

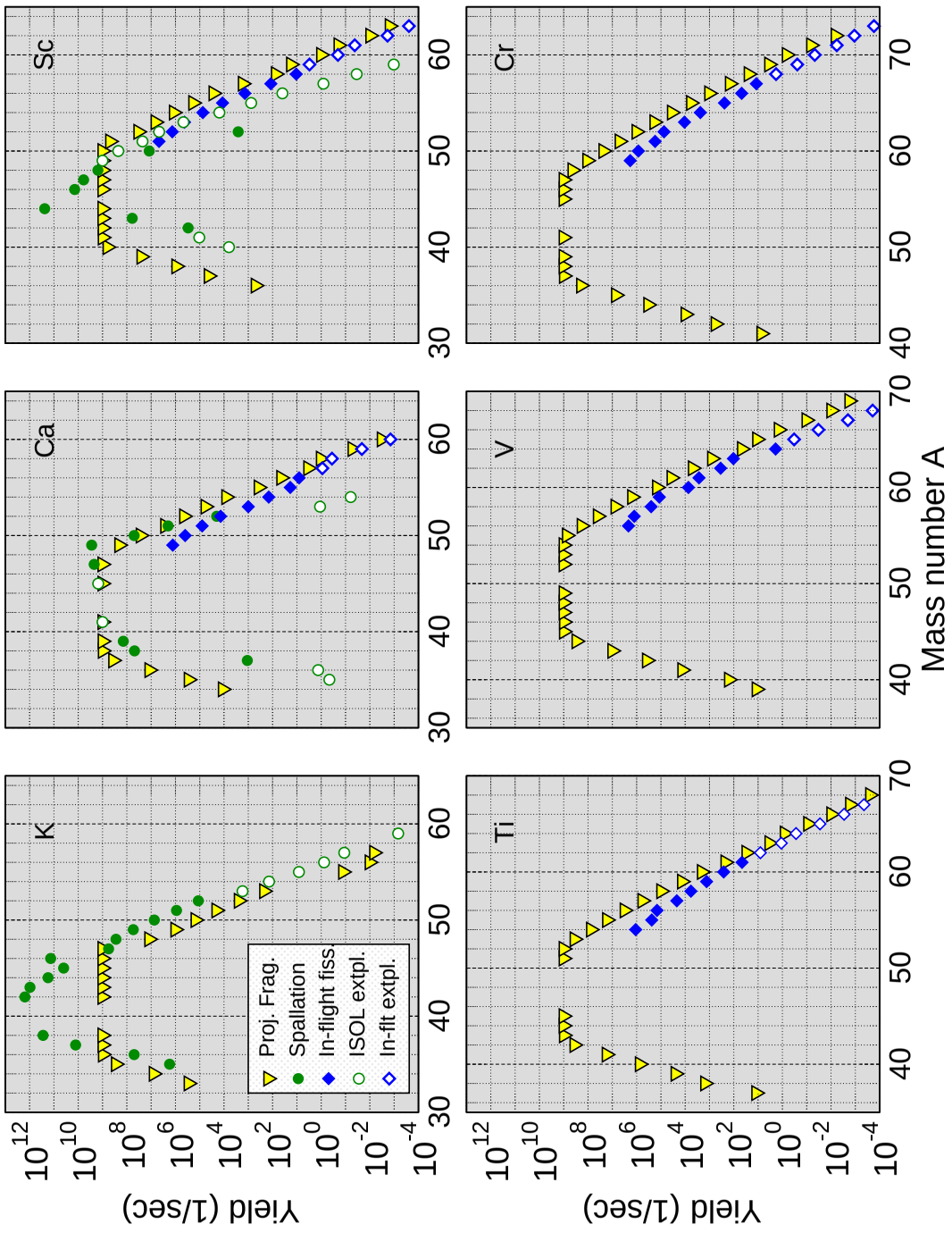

FIG. 10: Production rates of K, Ca, Sc, Ti, V, Cr 1^+-ions in a 200 MeV/u 400 kW machine.

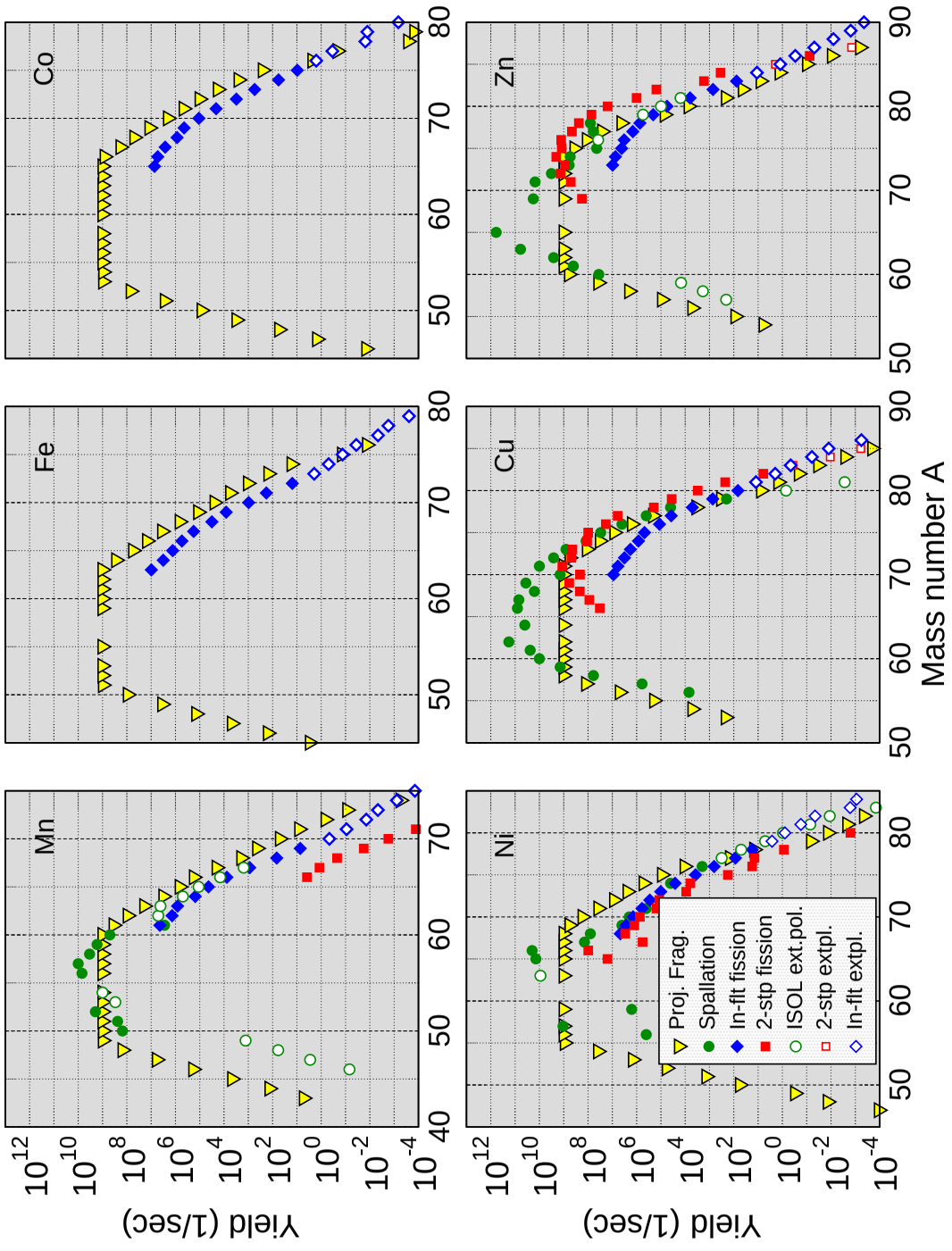

FIG. 11: Production rates of Mn, Fe, Co, Ni, Cu, Zn 1^+-ions in a 200 MeV/u 400 kW machine.

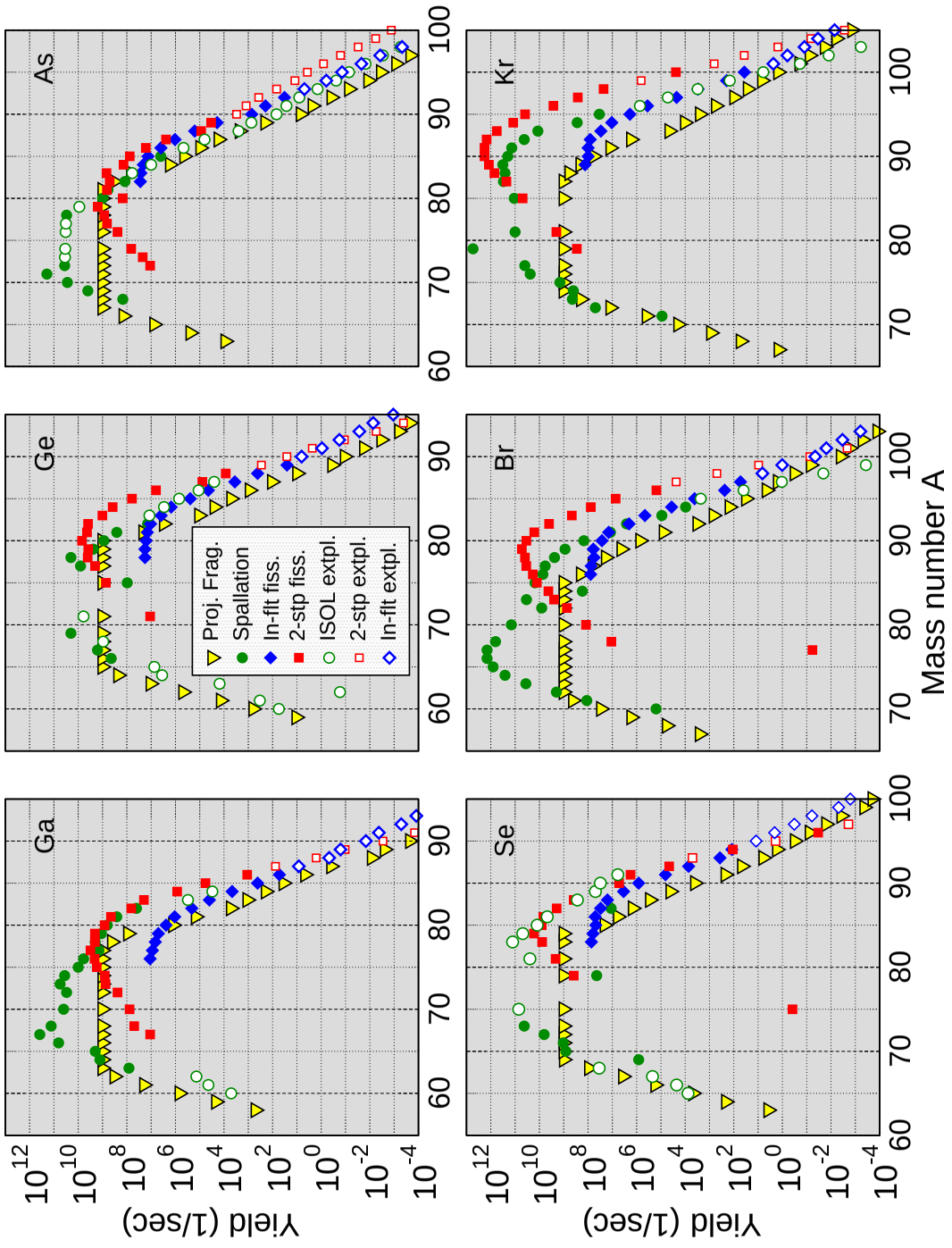

FIG. 12: Production rates of Ga, Ge, As, Se, Br, Kr 1^+-ions in a 200 MeV/u 400 kW machine.

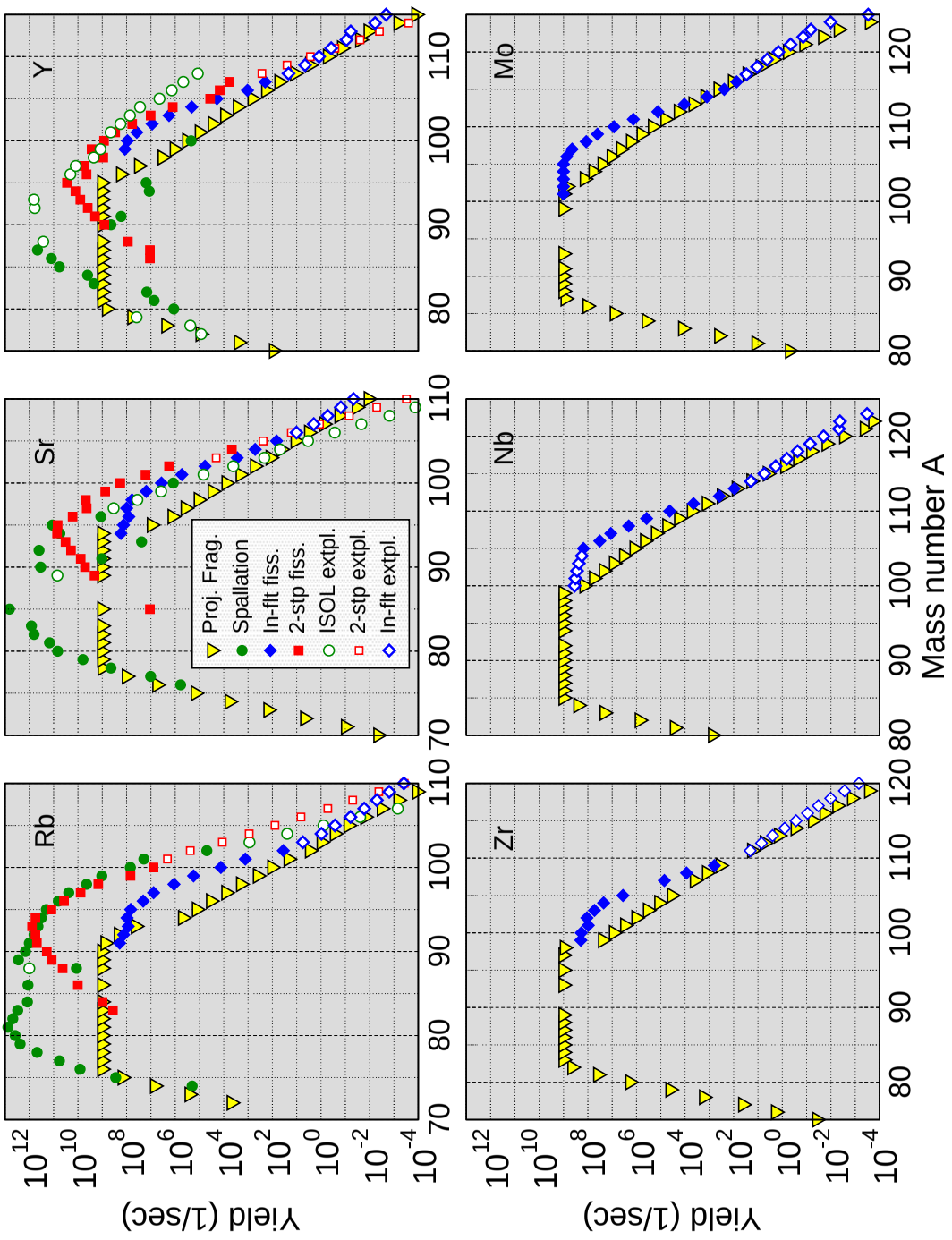

FIG. 13: Production rates of Rb, Sr, Y, Zr, Nb, Mo 1^+-ions in a 200 MeV/u 400 kW machine.

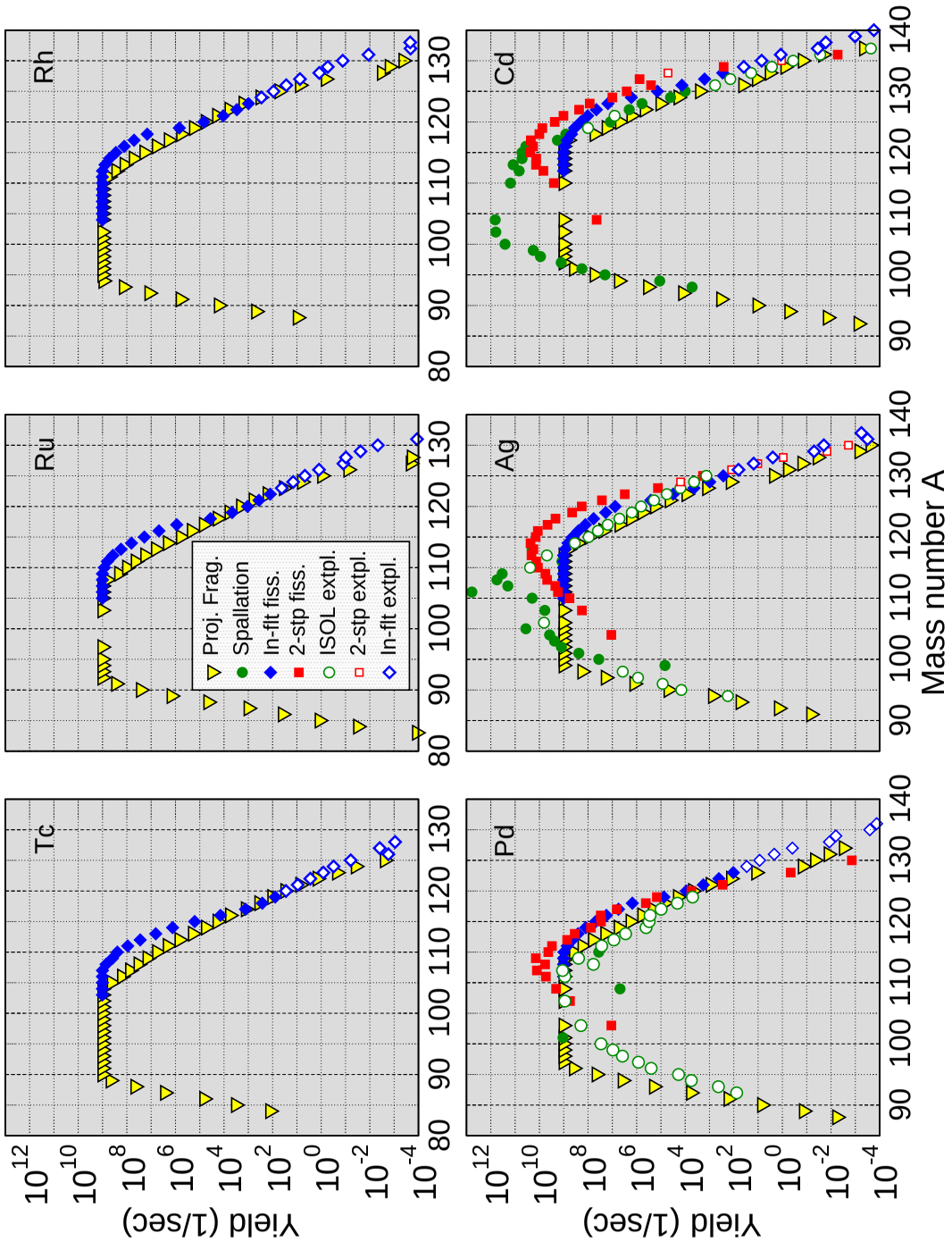

FIG. 14: Production rates of Tc, Ru, Rh, Pd, Ag, Cd 1^+-ions in a 200 MeV/u 400 kW machine.

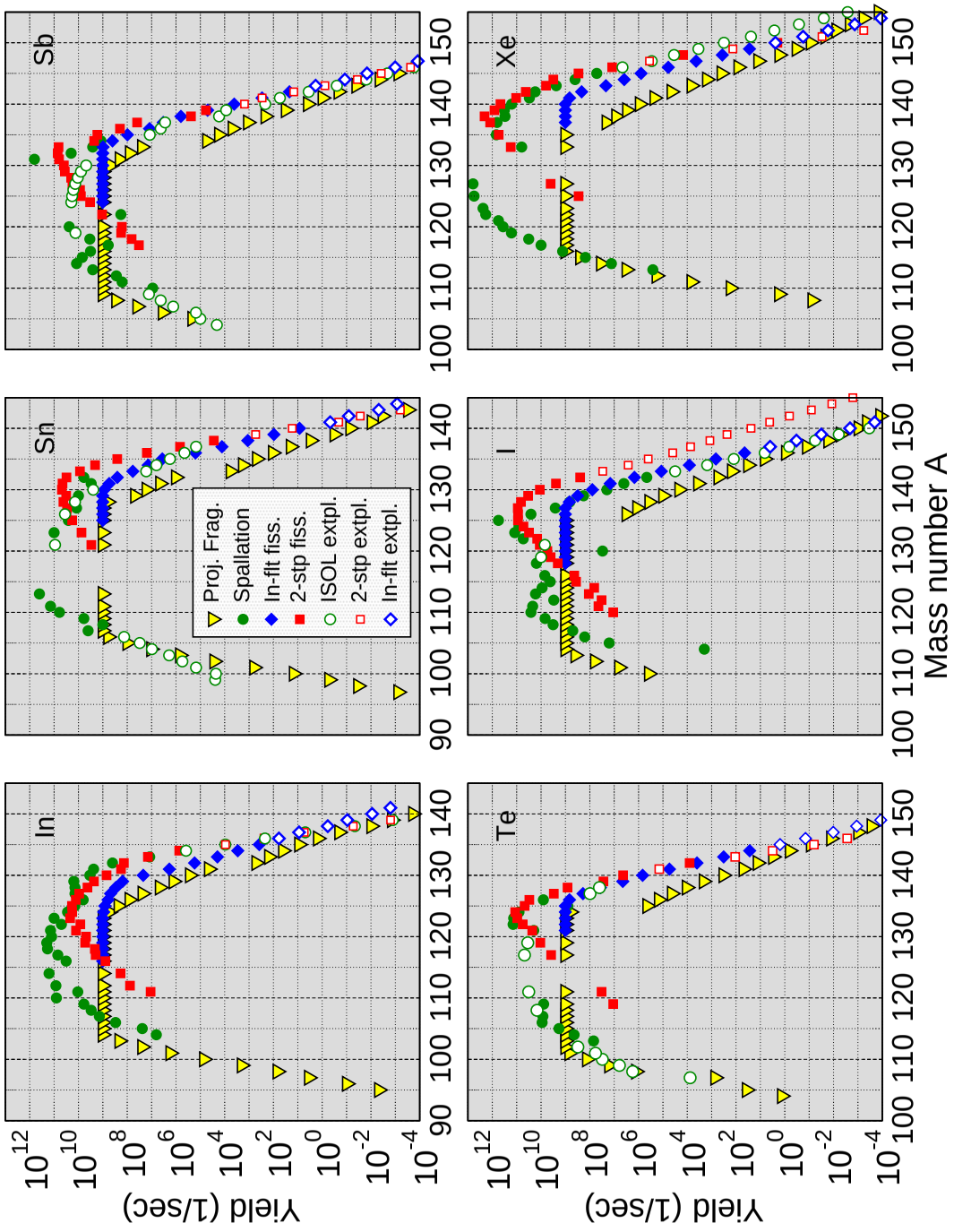

FIG. 15: Production rates of In, Sn, Sb, Te, I, Xe 1^+-ions in a 200 MeV/u 400 kW machine.

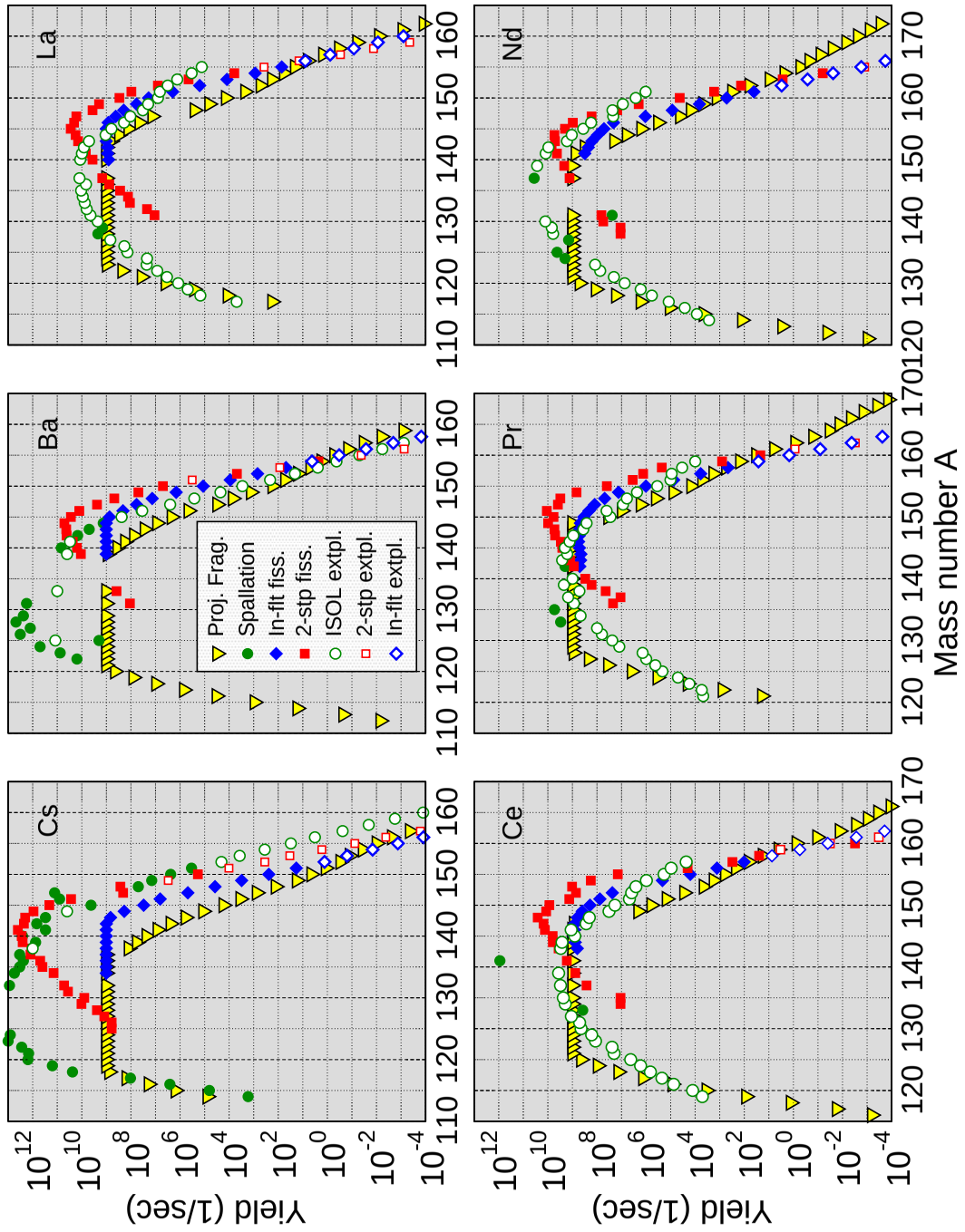

FIG. 16: Production rates of Cs, Ba, La, Ce, Pr, Nd 1^+-ions in a 200 MeV/u 400 kW machine.

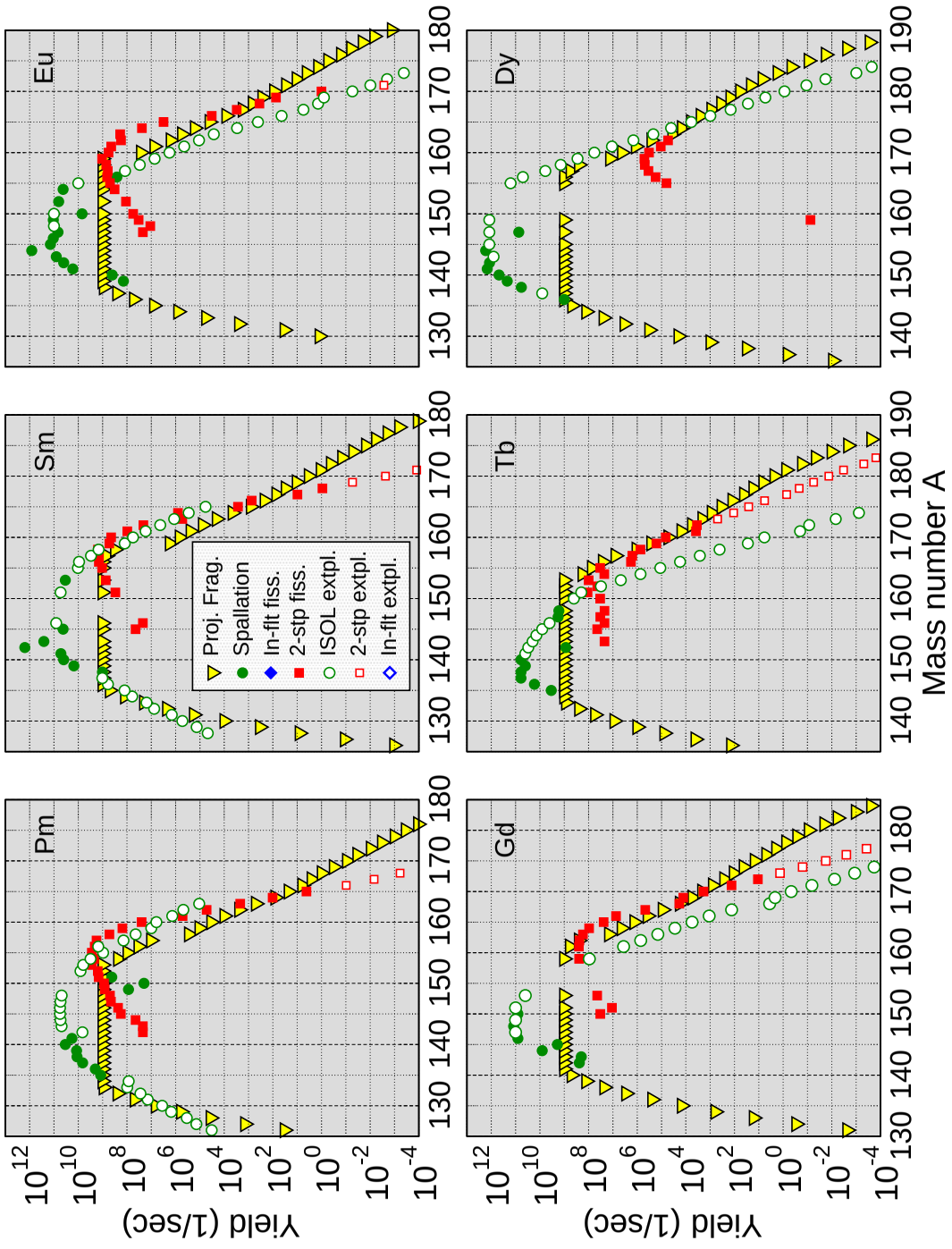

FIG. 17: Production rates of Pm, Sm, Eu, Gd, Tb, Dy 1^+-ions in a 200 MeV/u 400 kW machine.

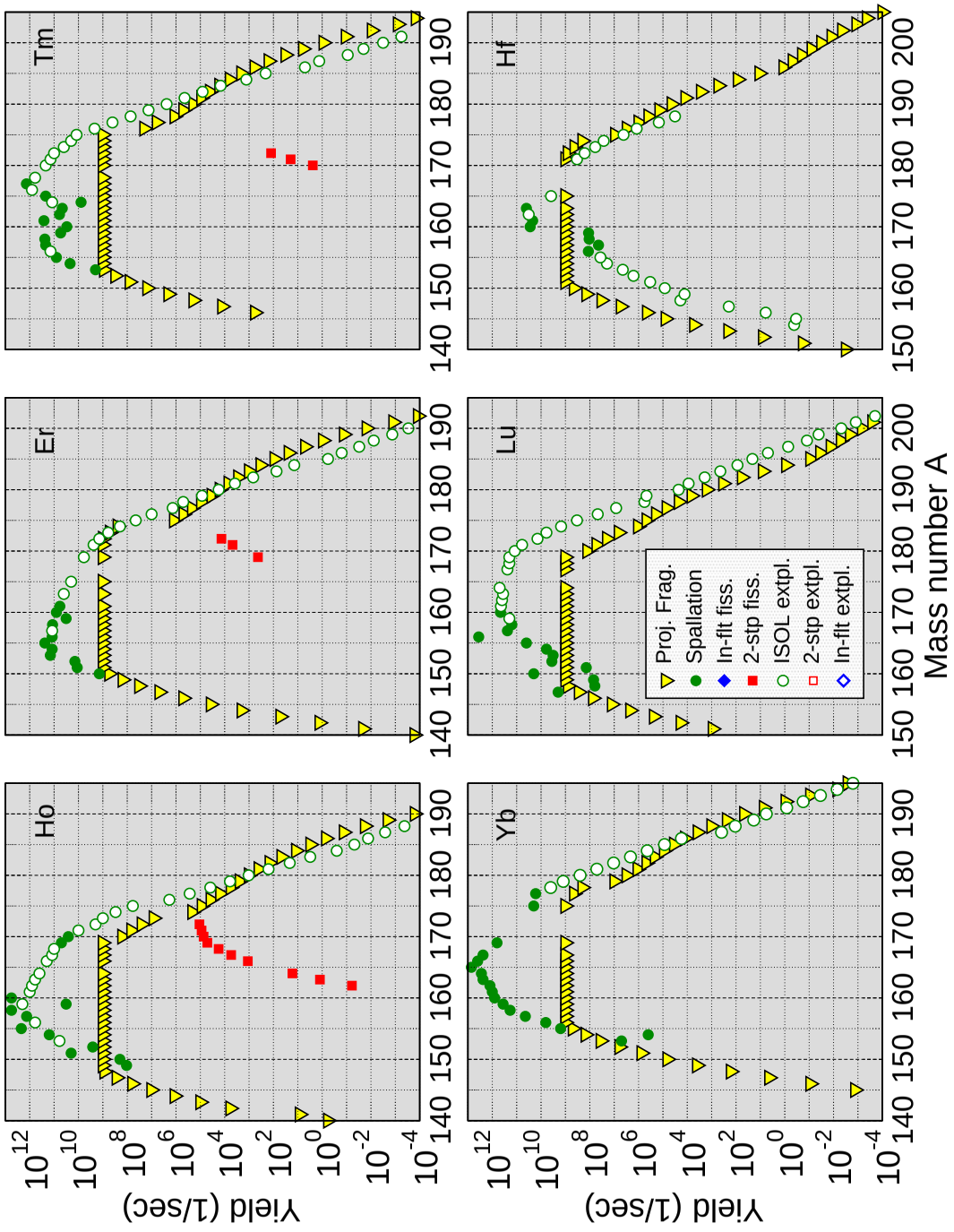

FIG. 18: Production rates of Ho, Er, Tm, Yb, Lu, Hf 1^{+}-ions in a 200 MeV/u 400 kW machine.

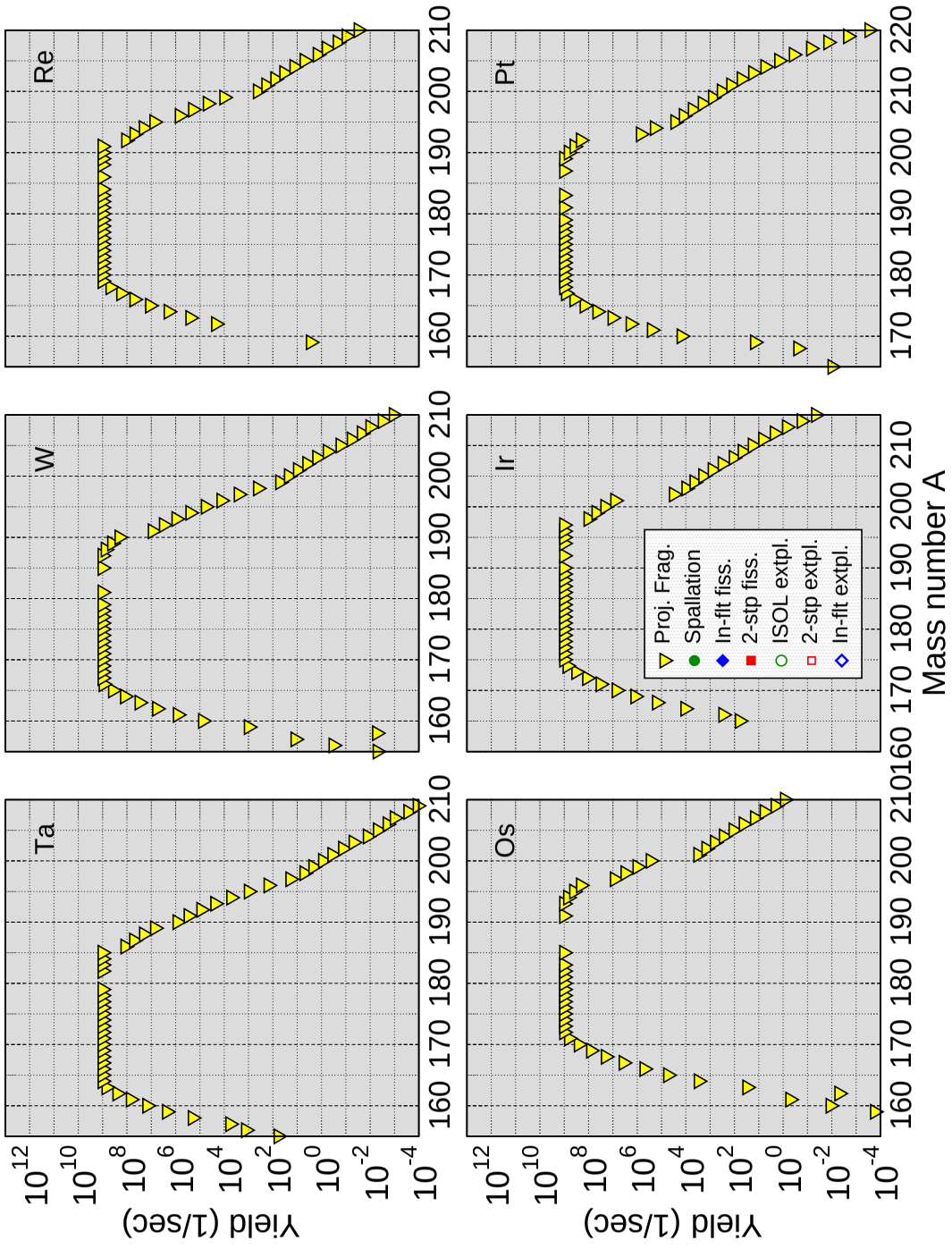

FIG. 19: Production rates of Ta, W, Re, Os, Ir, Pt 1^+-ions in a 200 MeV/u 400 kW machine.

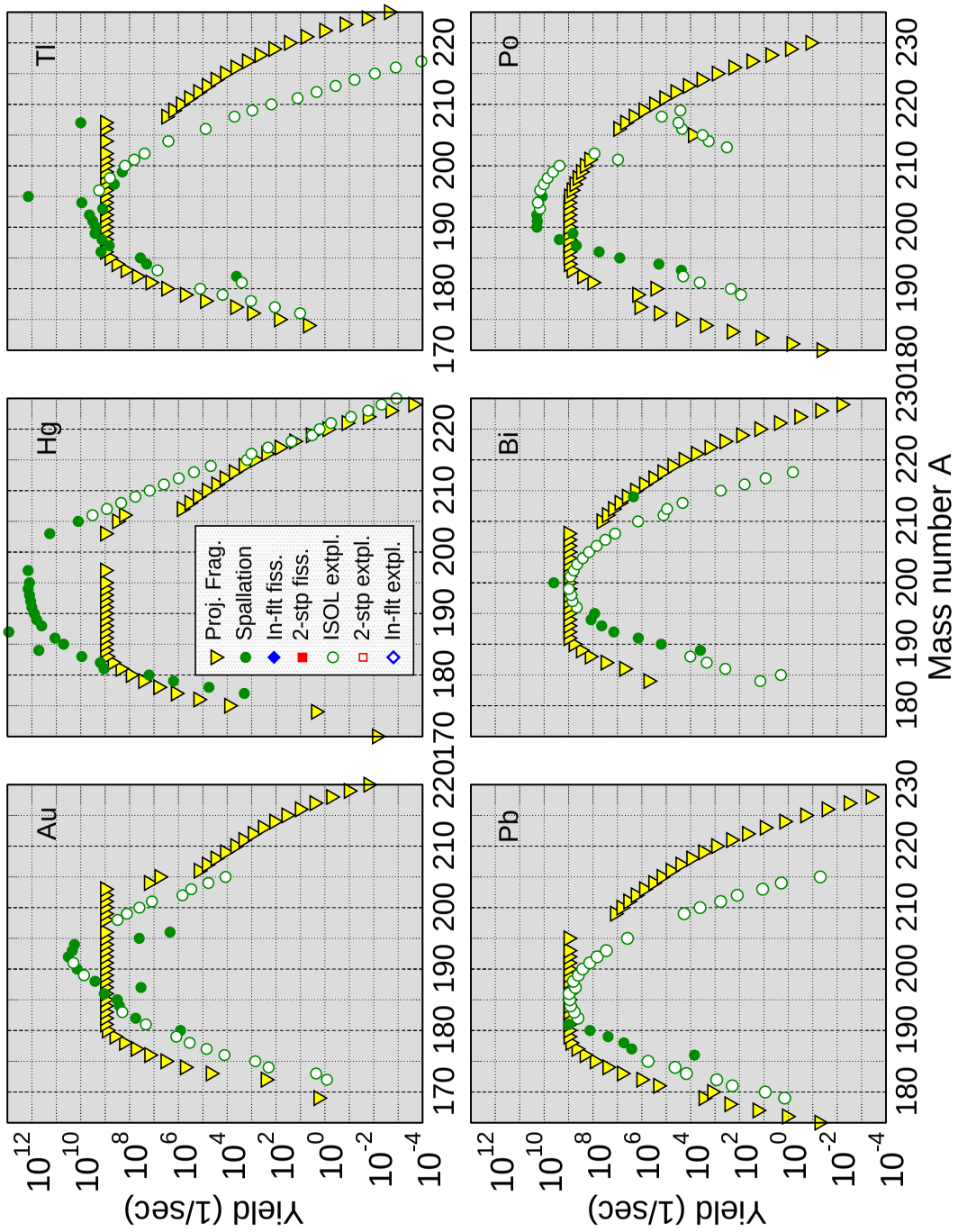

FIG. 20: Production rates of Au, Hg, Tl, Pb, Bi, Po 1^{+}-ions in a 200 MeV/u 400 kW machine.

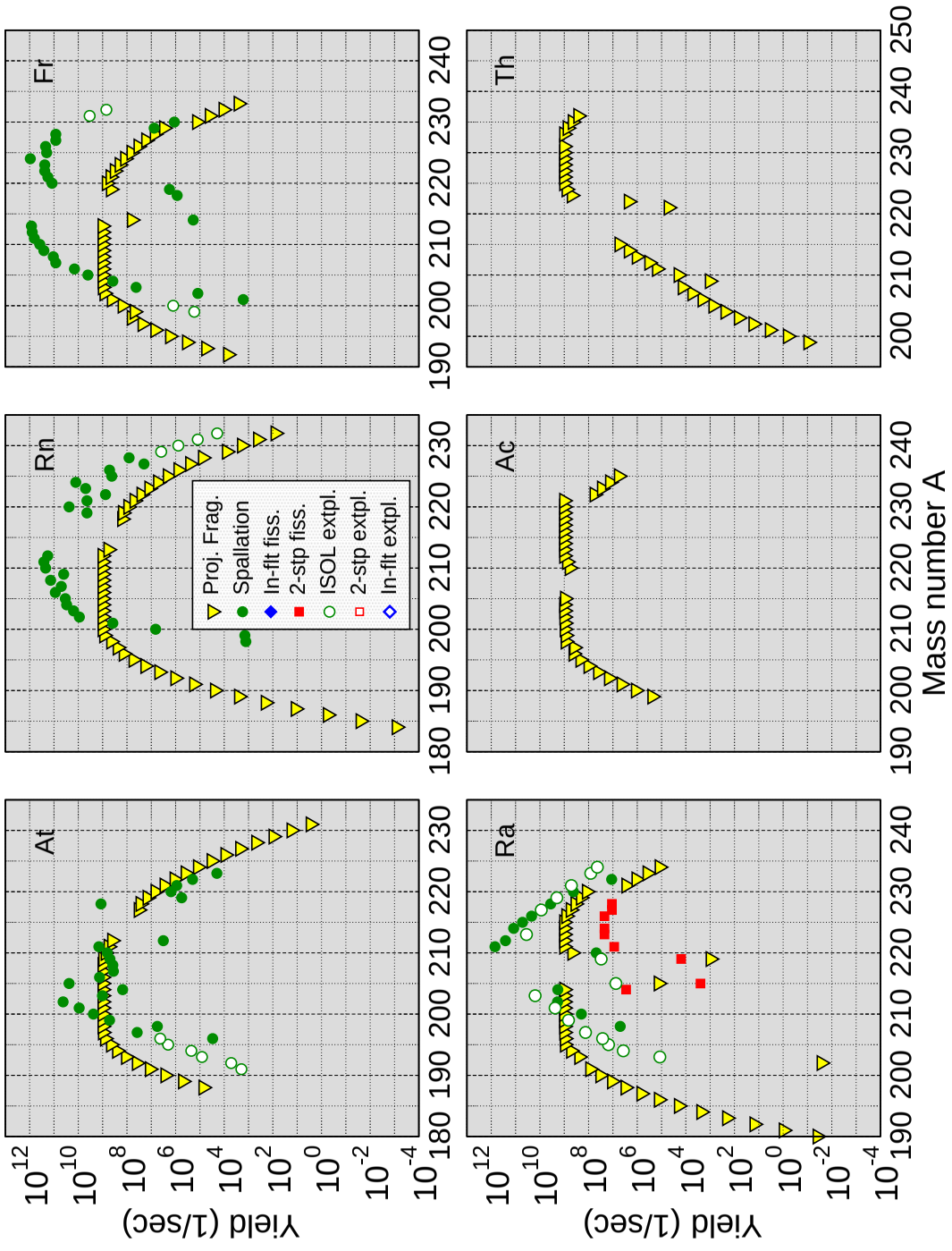

FIG. 21: Production rates of At, Rn, Fr, Ra, Ac, Th 1^+-ions in a 200 MeV/u 400 kW machine.

Physics Division
Argonne National Laboratory
9700 South Cass Avenue, Bldg. 203
Argonne, IL 60439-4843

www.anl.gov

UChicago ▶ Argonne LLC

A U.S. Department of Energy laboratory managed by UChicago Argonne, LLC